

A GENERALIZED DONSKER-KAČ FORMULA TO COMPUTE THE FUNDAMENTAL MODES IN COMPLEX LOADED WAVEGUIDES

Vincenzo Galdi
Vincenzo Pierro
Innocenzo M. Pinto
D.I.I.I.E., University of Salerno
via Ponte Don Melillo, I-84084 Fisciano (SA), Italy
E-mail: pinto@vaxsa.csied.unisa.it

Abstract

We present a novel algorithm for determining the fundamental modes and cutoff wavenumbers in metallic waveguides with arbitrary cross-section, possibly loaded with inhomogeneous dielectrics. The method is based upon a generalized Donsker-Kač formula which leads to a closed-form expression for the sought quantities in terms of asymptotic generalized Wiener-Itô integrals. These *path integrals* are computed by means of Monte Carlo methods, leading to a completely parallel algorithm with mild memory requirements. The method can be easily generalized to 3D problems including electromagnetic resonators.

1 - INTRODUCTION.

The computation of modal fields in complex, longitudinally uniform, conducting (possibly loaded) waveguides and of their corresponding cutoff wavenumbers is an important problem in microwave theory and applications and has been widely studied in the past. Unfortunately, analytical solutions are available only for few (separable) geometries. In the last decade a great effort was devoted to the development of numerical techniques which allow to analyze arbitrary-shaped structures, possibly filled by an inhomogeneous medium with complicated refraction index distribution. Most of these techniques are conceptually amenable to Finite Elements Methods (Silvester and Ferrari, 1990) or Methods of Moments (Harrington, 1968) (henceforth FEM and MoM, respectively). They require meshing algorithms (FEM) or a choice of basis functions (MoM), which could become quite demanding in the presence of wildly irregular boundaries. Moreover they could be relatively expensive in terms of storage and CPU requirements. However, in many applications one is interested only in the fundamental modes. In this connection we introduced recently a new class of numerical methods, based on Functional Integration and Monte Carlo methods (Galdi et al., 1997), which could

provide an attractive alternative to the usual techniques in terms of power, ease of application and computational budget. In this paper we discuss the new algorithm for computing the dominant modes and cutoff wavenumbers in complex loaded waveguides, based on a generalized Donsker-Kač (henceforth GDK) formula and Monte Carlo method, in a rather general form. The paper is organized as follows. In *Section 2* we introduce the GDK formula in connection with the general Helmholtz eigenvalue problem. In *Section 3* we discuss an efficient and powerful strategy to compute the involved functional integrals. In *Section 4* we present some interesting computational results, compared with some known exact and approximate solutions. In *Section 5* we highlight the computational features of the proposed method by comparison with MoM and FEM. Conclusions follow in *Section 6*. A number of formal developments and ancillary concepts are collected in the Appendices.

2 - BASIC THEORY.

Let:

$$L = \frac{1}{2} \sum_{i,j=1}^n b^{ij} \frac{\partial^2}{\partial x^i \partial x^j} + \sum_{i=1}^n a^i \frac{\partial}{\partial x^i} \quad (1)$$

an n -dimensional second order linear differential operator on a compact subset $\mathcal{D} \subseteq R^n$ of regular boundary $\partial\mathcal{D}$. The associated Helmholtz eigenvalue problem is considered:

$$\begin{cases} L\phi(\underline{x}) - [V(\underline{x}) - \lambda] \phi(\underline{x}) = 0 & , \quad \underline{x} \in \mathcal{D}, \\ \phi(\underline{x}) = 0 \quad \left(\frac{\partial \phi}{\partial n}(\underline{x}) = 0 \right) & , \quad \underline{x} \in \partial\mathcal{D}, \end{cases} \quad (2)$$

with homogeneous Dirichlet (Neumann) boundary conditions, V being a regular function. It is well known that the problem (2) has a discrete spectrum of real eigenvalues (Ray, 1954), $\lambda_1 < \lambda_2 < \lambda_3 < \dots$, and associated eigenfunctions ϕ_j , $j = 1, 2, 3, \dots$ forming an orthonormal system in $L^2(\mathcal{D})$, (Reed and Simon, 1975).

The Donsker-Kač Formula (Donsker and Kač, 1950), exploited in (Galdi et al., 1997) for computing the lowest eigenvalue (eigenfunction) of the problem (2) with $\mathcal{D} = R^n$ and regularity-at-infinity conditions (dielectric waveguides), can be generalized to bounded domains and Dirichlet (Neumann) boundary conditions (see Appendix A), yielding:

$$\lambda_1 \sim (T_2 - T_1)^{-1} \log \left\{ \frac{E_{\underline{x}} \left[f[\underline{\xi}(T_1)] \exp \left\{ - \int_0^{T_1} V[\underline{\xi}(s)] ds \right\} \right]}{E_{\underline{x}} \left[f[\underline{\xi}(T_2)] \exp \left\{ - \int_0^{T_2} V[\underline{\xi}(s)] ds \right\} \right]} \right\} , \quad T_2 > T_1 \quad (3)$$

$$\phi_1(\underline{x}) \sim C E_{\underline{x}} \left[f[\underline{\xi}(T)] \exp \left\{ - \int_0^T V[\underline{\xi}(s)] ds \right\} \right], \quad (4)$$

where C is a normalization constant and the equality holds for $T, T_1, T_2 \rightarrow \infty$. The symbol $E_{\underline{x}}$ represents a *Functional Integral* (expectation value) on the probability measure associated to the Itô process $\underline{\xi}(s)$ of initial point $\underline{x} = (x^1, \dots, x^n)$, generated (Ventsel, 1983) by the operator L under *absorption* (Dirichlet boundary conditions) or *reflection* (Neumann boundary conditions) at the boundary $\partial\mathcal{D}$ (Gihman and Skorohod, 1972; Gerardi et al., 1984), and f is a suitable *weight* function (see Appendix A). The Itô process $\underline{\xi} = (\xi^1, \dots, \xi^n)$, in the domain \mathcal{D} is ruled by the following stochastic integral equation (Gihman and Skorohod, 1972; Gardiner, 1983):

$$\xi^i(s) = x^i + \int_0^s a^i[\underline{\xi}(\tau)] d\tau + \sum_{j=1}^n \int_0^s \sqrt{b^{ij}[\underline{\xi}(\tau)]} dw_{\tau}^j, \quad (5)$$

$$0 \leq s \leq T, \quad i = 1, \dots, n,$$

$\{dw_{\tau}^i\}_{i=1, \dots, n}$ being independent one-dimensional Wiener differentials (see Appendix B).

3 - NUMERICAL IMPLEMENTATION.

The previous Section has shown that use of GDK formula reduces the computation of the lowest order eigenvalues and eigenfunctions to that of generalized¹ Wiener-Itô functional integrals. Though *exotic* at first glance, this approach exhibits several nice features. In fact, the computation of the needed functional integrals can be carried out by means of Monte Carlo methods, leading to an intrinsically parallel algorithm, with a computational burden growing only linearly with both problem size (characteristic-dimension/wavelength) and spatial embedding dimension. Moreover, as previously noted, memory requirements are practically negligible and meshing algorithms and/or basis functions choice issue are avoided. Finally, there are *no* severe restrictions on the geometrical and/or constitutive complexity of the structure, provided the problem is scalar(izable).

In this Section the problem of computing the Wiener-Itô integral of a regular functional $g[\underline{\xi}(\cdot), T]$ is addressed. In our special case we have:

$$g[\underline{\xi}(\cdot), T] = f[\underline{\xi}(T)] \exp \left\{ - \int_0^T V[\underline{\xi}(s)] ds \right\}. \quad (6)$$

The underlying idea can be explained as follows. First, a piecewise-linear time discretization is introduced with (e.g. constant) step size Δ . Next, one

¹In view of the imposed boundary conditions.

resorts to the classical discrete-time *Euler approximation* for the involved Itô process (Kloeden and Platen, 1991):

$$\xi^i(t_k) = x^i + a^i[\underline{\xi}(t_{k-1})] \Delta + \sum_{j=1}^n \sqrt{b^{ij}[\underline{\xi}(t_{k-1})]} \Delta_{Wk}^i, \quad (7)$$

$$0 \leq t_{k-1}, t_k \leq T, \quad i = 1, \dots, n,$$

where $t_k - t_{k-1} = \Delta$, $t_0 = 0$, and Δ_{Wk}^i are independent gaussian distributed random variables with means and variances:

$$E[\Delta_{Wk}^i] = 0, \quad E[(\Delta_{Wk}^i)^2] = \Delta. \quad (8)$$

The process is evolved, using eq. (3), until it hits the boundary. Then it can have two different evolutions, depending on the boundary conditions (see Appendix A). The behaviours are clearly explained in *Fig. 1*:

- Dirichlet boundary condition \Rightarrow *absorption at the boundary*;
- Neumann boundary condition \Rightarrow *reflection at the boundary*.

Combinations of absorption and (possibly delayed) reflection can be used to model more complex (mixed) boundary conditions (Gerardi et al., 1984). The process is finally stopped when $t_k = T$. Following the classical Monte Carlo scheme (Sobol, 1975), it is possible to compute the functional integral $E[g[\underline{\xi}(\cdot), T]]$ by iterating the above procedure and evaluating the arithmetic means:

$$\mu_1(M, \Delta) = M^{-1} \sum_{h=1}^M \hat{g}[\underline{\xi}(t_0)^{(h)}, \dots, \underline{\xi}(T)^{(h)}; T], \quad (9)$$

$$\mu_2(M, \Delta) = M^{-1} \sum_{h=1}^M \left\{ \hat{g}[\underline{\xi}(t_0)^{(h)}, \underline{\xi}(t_1)^{(h)}, \dots, \underline{\xi}(T)^{(h)}; T] \right\}^2. \quad (10)$$

where the symbol \hat{g} denotes the function obtained by evaluating the functional g on the piecewise-linear path $\{\underline{\xi}(t_0)^{(h)}, \underline{\xi}(t_1)^{(h)}, \dots, \underline{\xi}(T)^{(h)}\}$ and the superfix (h) labels the h^{th} realization of the random path. The sought functional integral can be accordingly computed as:

$$E[g[\underline{\xi}(\cdot), T]] = \lim_{\Delta \rightarrow 0} \lim_{M \rightarrow \infty} \mu_1(M, \Delta). \quad (11)$$

Obviously, for finite values of Δ, M the estimation will be affected by:

- a systematic error, due to the effect of time-discretization, $\epsilon_{sys} \sim \mathcal{O}(\Delta)$;

- a statistical error, which in view of the Central Limit theorem is asymptotically gaussian, with zero average and r.m.s. deviation (Sobol, 1975; Klocden and Platen, 1991):

$$\epsilon_{stat} \sim \left\{ M^{-1} \text{var}[g(\xi(\cdot), T)] \right\}^{1/2},$$

which depends on Δ (weakly), as well as on M (strongly).

The confidence interval of the estimated functional integral is thus:

$$\delta(M, \Delta) = \mu_1(M, \Delta) \pm \alpha M^{-1/2} [\mu_2(M, \Delta) - \mu_1^2(M, \Delta)]^{1/2}, \quad (12)$$

where α depends of the sought confidence level. Systematic and statistical errors associated to formulas (3), (4) can be readily estimated using standard error propagation formulas.

4 - ILLUSTRATIVE EXAMPLES.

The first example of application refers to an homogeneous circular coaxial waveguide. This example has been chosen because the analytical solution is known (Collin, 1992), thus allowing the evaluation of the obtained accuracy. The associated eigenvalue problem is (Collin, 1992):

$$\begin{cases} \nabla_t^2 \phi(x, y) + k_c^2 \phi(x, y) = 0, & (x, y) \in \mathcal{D}, \\ \phi(x, y) = 0, & (x, y) \in \partial \mathcal{D} \quad , \quad \text{TM modes}, \\ \frac{\partial \phi}{\partial n}(x, y) = 0, & (x, y) \in \partial \mathcal{D} \quad , \quad \text{TE modes}, \end{cases} \quad (13)$$

where the symbol ∇_t^2 is the transverse Laplacian and k_c represents the cutoff wavenumber. This problem is easily recognized to belong to the general class (2) considered in *Section 2*, so that the GDK formula can be applied to compute the first TE, TM modes. In *Fig. 2* the exact and computed cutoff wavelength:

$$\lambda_c = \frac{2\pi}{k_c},$$

(scaled with respect to a characteristic dimension) versus the ratio between the inner and outer coaxial radii are compared for the fundamental TE and TM modes. The accuracy obtained in the calculation is better illustrated in *Fig. 3*, where the computed errors (circles) are displayed, and shown to be much smaller than the corresponding confidence-interval halfwidths (squares) evaluated from eq. (12), being always $\leq 1\%$. *Fig. 4* shows the

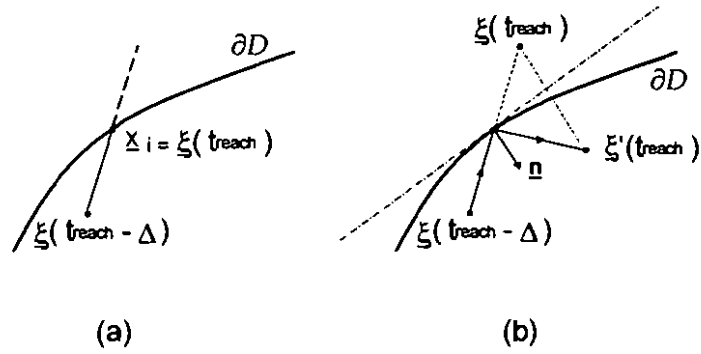


FIGURE 1 - Enforced behaviours of the Itô process at the boundary.
 (a) Dirichlet boundary conditions: $\xi(t) = \underline{x}_i$ for $t \geq t_{reach}$.
 (b) Neumann boundary conditions: the process is mirror reflected after hitting the boundary, $\xi'(t_{reach}) \rightarrow \xi(t_{reach})$.

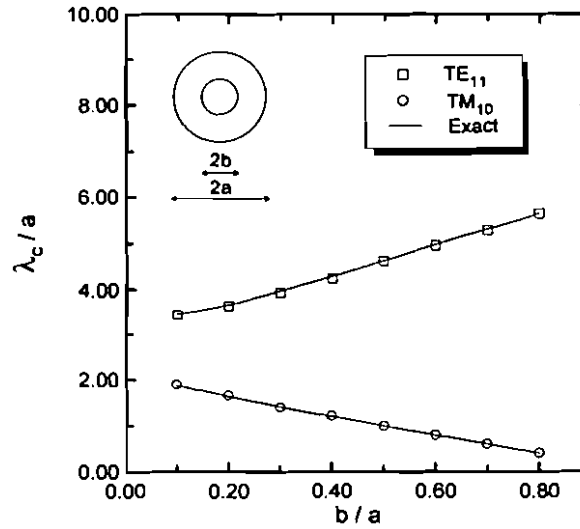


FIGURE 2 - Coaxial circular waveguide. Scaled cut-off wavelength vs. b/a (fundamental TE and TM modes). Continuous line: exact solution; markers: GDK method.

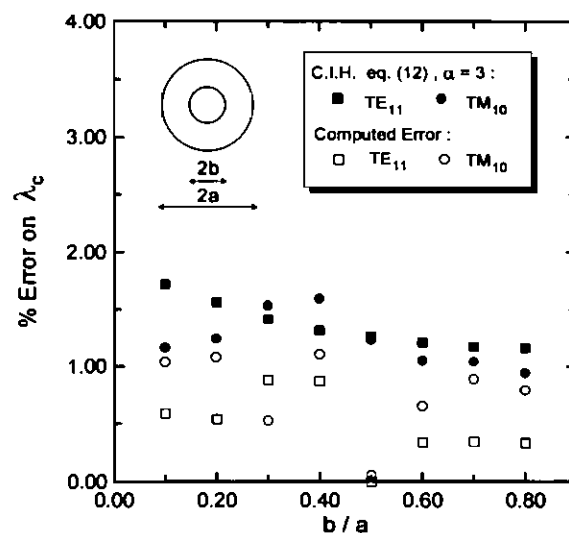


FIGURE 3 - Computed errors and estimated confidence halfwidths pertinent to FIGURE 2.

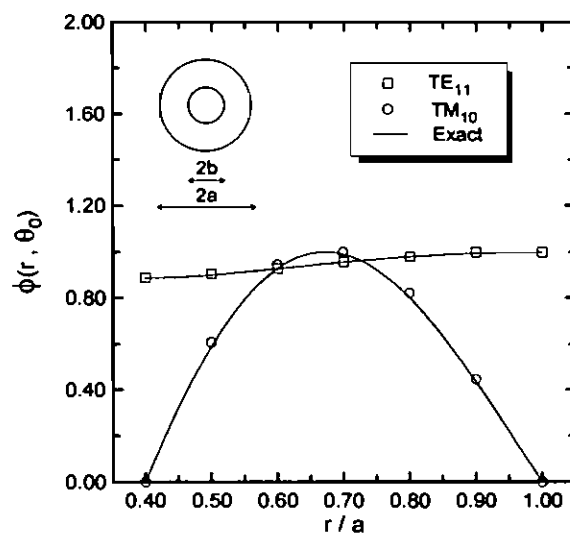


FIGURE 4 - Coaxial circular waveguide. Radial behaviour of the fundamental TE and TM modes at a fixed azimuthal angle ($\Theta_0 = \pi/2$, $b/a = 0.4$). Continuous line: exact solution; markers: GDK method.

comparison between the corresponding exact and computed eigenfunctions. It can be seen that the agreement is very good.

As a further example, a homogeneous rectangular waveguide is considered with a double (symmetrical) ridge. For such a structure no analytical solutions are available, but there exist several approximations. One of the most popular approximations (see, e.g. Collin, 1992) is based on the transverse resonance method and quasistatic conformal mapping. In *Fig. 5* the GDK computed scaled cutoff wavelength (as a function of the scaled ridge width, at several values of the ridge spacing) is compared to the one obtained from the above approximation, for the fundamental (quasi-TE₁₀) mode. Also in this case there is a very good agreement. *Fig. 6* shows the behaviour of the corresponding eigenfunction.

Finally, an inhomogeneous structure is considered, namely a rectangular waveguide loaded with a dielectric slab (see *Fig. 7*). In this case analytical solutions are easily obtained by applying the transverse resonance technique (Collin, 1960). The eigenvalue problem is (Collin, 1960):

- LSE_{nm} modes:

$$\begin{cases} \frac{d^2}{dx^2}\phi(x) + \left\{ k_0^2 [n^2(x) - n_1^2] - h^2 - \left(\frac{m\pi}{b}\right)^2 \right\} \phi(x) = 0, & 0 < x < a, \\ \phi(x) = 0, & x = 0, a, \end{cases} \quad (14)$$

- LSM_{nm} modes:

$$\begin{cases} \left[\frac{d^2}{dx^2} - \frac{1}{n^2(x)} \frac{dn^2(x)}{dx} \frac{d}{dx} \right] \phi(x) + \left\{ k_0^2 [n^2(x) - n_1^2] - h^2 - (m\pi/b)^2 \right\} \phi(x) = 0, & 0 < x < a, \\ \frac{d}{dx}\phi(x) = 0, & x = 0, a, \end{cases} \quad (15)$$

where k_0 indicates the free-space wavenumber and $n^2(x)$ the transverse dielectric profile. The symbol h denotes the so-called *modal parameter*:

$$h^2 = k_0^2 n_1^2 - \left(\frac{m\pi}{b}\right)^2 - \beta^2, \quad (16)$$

β being the propagation constant. It is clearly seen that modal cutoff occurs when

$$h^2 = k_0^2 n_1^2 - \left(\frac{m\pi}{b}\right)^2. \quad (17)$$

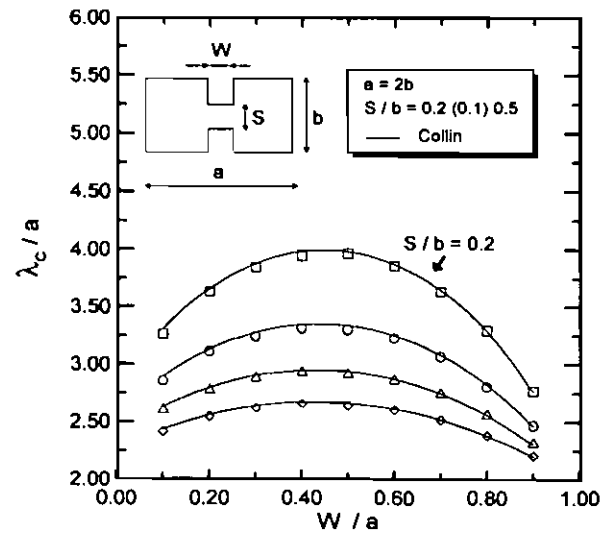


FIGURE 5 - Double-ridge waveguide. Scaled cut-off wavelength vs. scaled ridge-width (TE fundamental mode) at various S/b values. Continuous line: std. solution (Collin, 1992, p. 205); markers: GDK method.

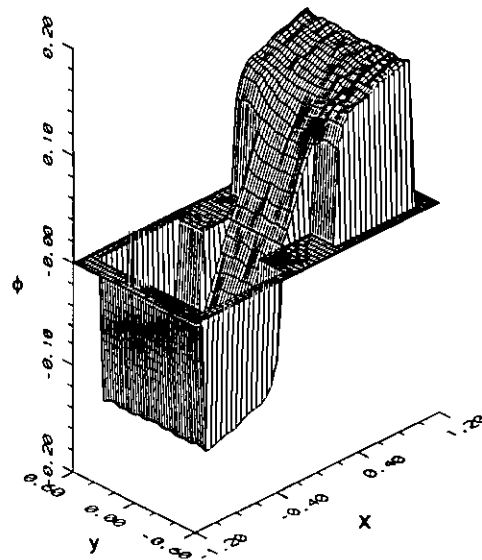


FIGURE 6 - Double-ridge waveguide. TE fundamental mode. ($a = 2b = 2$, $W/a = 0.3$, $S/b = 0.5$.)

As one can easily see, also these problems belong to the class (2) analyzed in *Section 2*, and thus it is possible to use the GDK formula. In *Figs 7, 8* the exact dispersion curves (scaled modal parameter versus scaled free-space wavenumber) are reported, together with the GDK computed values for the fundamental LSE, LSM modes ². In this case one also notes the very good agreement.

In order to obtain all the above results, a typical value of M is 10^5 , with an adaptive time-step ($\Delta \sim 10^{-5}$ close to the boundary, where the evolution of the path is more critical; $\Delta \sim 10^{-3}$ elsewhere). It was observed that values of T_1, T_2 such that $k_c^2 T_{1,2} > 2$, k_c^2 being the estimated eigenvalue, guarantee that the truncation error (see Appendix A) does not affect appreciably the overall accuracy. This condition can be (and actually has been) easily imposed using a simple adaptive scheme.

5 - COMPUTATIONAL FEATURES.

The main computational features (merits and drawbacks) of the proposed GDK-Monte-Carlo method (henceforth GDKMC), emphasized in the previous Sections, as compared to standard methods (e.g. FEM, MoM), can be summarized as follows

- GDKMC implementation is straightforward, irrespective of the complexity of the structure. Meshing algorithms and basis functions are unnecessary.
- GDKMC storage requirements are practically negligible. In contrast FEM, MoM require usually the storage of *large* matrices.
- GDKMC computational burden grows *only* linearly with *both* problem size (characteristic-length/wavelength) *and* spatial embedding dimension n .
- GDKMC is intrinsically a parallel processing algorithm. In fact all repeated operations (path generation, functional evaluation) can be performed without any mutual interaction and so can be easily and fully distributed among parallel processors.
- GDKMC has a rather slow (statistical, $\propto M^{-1/2}$) convergency rate. By comparison with the standard methods, however, it could be not significantly slower, especially for very complex structures. Tight accuracy bounds are easily obtained.

²As a technical hint, note that the diffusion operator related to LSM modes contains a derivative of the refraction index profile which, in this case, become singular at the interfaces (step index profile). To avoid this problem a *trapezoidal approximation* has been used for the pertinent step profile.

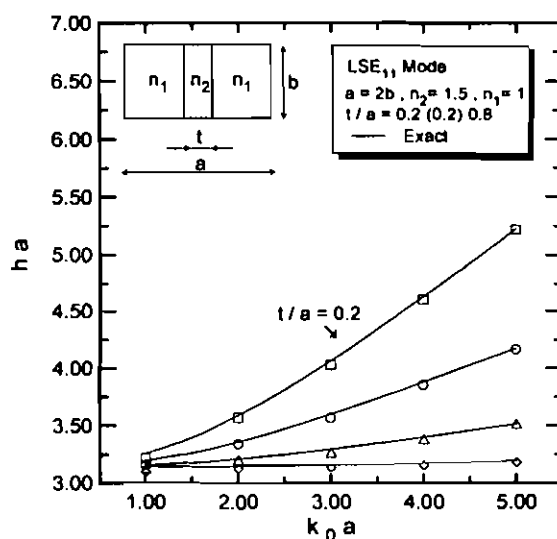


FIGURE 7 - Dielectric loaded rectangular waveguide. LSE₁₁ mode dispersion diagram at various values of dielectric slab thickness. Continuous line: exact solution; markers: GDK method.

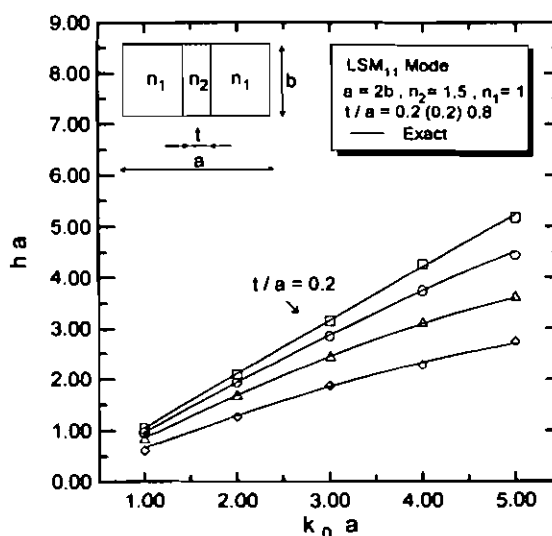


FIGURE 8 - Dielectric loaded rectangular waveguide. LSM₁₁ mode dispersion diagram at various values of dielectric slab thickness. Continuous line: exact solution; markers: GDK method.

- GDKMC permits an easy computation of the fundamental modes in scalar(izable) problems *only*.

As a conclusion one can state that GDKMC is particularly suited for the analysis of structures with complicated geometries and/or constitutive properties, whenever one is interested only in the fundamental modes, and fast computing engines (possibly parallel) and relatively little memory are available.

6 - CONCLUSIONS AND RECOMMENDATIONS.

A new algorithm has been developed for computing the lowest order modes in arbitrary shaped inhomogeneous waveguides. The method is based upon a generalization of the DK formula, well-established in different contexts (e.g. quantum mechanics), and numerically implemented by means of Monte Carlo methods. A number of applications have been presented and the computed results have been compared with some known (exact and approximate) solutions showing good accuracy. A thorough evaluation of the computational features has been carried out, by comparison with traditional techniques (e.g. FEM, MoM). The proposed method turns out to be very versatile, easy to implement, and potentially advantageous with respect to traditional ones, in terms of computational budget. Hints for future research include:

- Extension to the computation of the (lowest order) resonant frequencies in 3D structures.
- Computation of higher order modes. In fact, in the presence of symmetrical structures, it is possible to exploit the symmetry of the eigenfunctions to *scale* the problem in the spectral domain (Donsker and Kač, 1950).

APPENDIX A - GDK FORMULA.

The elliptic eigenvalue problem introduced in *Section 1* is considered:

$$\begin{cases} L\phi(\underline{x}) - [V(\underline{x}) - \lambda] \phi(\underline{x}) = 0 & , \quad \underline{x} \in \mathcal{D}, \\ \phi(\underline{x}) = 0 \quad \left(\frac{\partial \phi}{\partial n}(\underline{x}) = 0 \right) & , \quad \underline{x} \in \partial \mathcal{D}, \end{cases} \quad (A1)$$

As well known in quantum mechanics, the associated parabolic (final value) problem:

$$\begin{cases} \frac{\partial \psi}{\partial t}(\underline{x}, t, T) = L\psi(\underline{x}, t, T) - V(\underline{x})\psi(\underline{x}, t, T) & , \quad \underline{x} \in \mathcal{D} & , \quad 0 \leq t < T, \\ \psi(\underline{x}, t, T) = 0 \quad \left(\frac{\partial \psi}{\partial n}(\underline{x}, t, T) = 0 \right) & , \quad \underline{x} \in \partial \mathcal{D} & , \quad 0 \leq t < T, \\ \psi(\underline{x}, T, T) = f(\underline{x}) & , \quad \underline{x} \in \mathcal{D}, \end{cases} \quad (A2)$$

admits the following exact solution³ (Feynman-Kač Formula, Gihman and Skorohod, 1972; Ventsel, 1983):

$$\psi(\underline{x}, t, T) = E_{\underline{x}} \left[f[\xi(T)] \exp \left\{ - \int_t^T V[\xi(s)] ds \right\} \right] & , \quad 0 \leq t \leq T, \quad (A3)$$

where $E_{\underline{x}}$ is a Functional Integral (expectation value) over the paths of the Itô process $\xi = (\xi^1, \dots, \xi^n)$, of initial point $\underline{x} = (x^1, \dots, x^n)$, generated by the operator L (Ventsel, 1983), ruled by the following stochastic equation (Gihman and Skorohod, 1972; Gardiner, 1983):

$$\begin{aligned} \xi^i(s) &= x^i + \int_t^s a^i[\xi(\tau)] d\tau + \sum_{j=1}^n \int_t^s \sqrt{b^{ij}[\xi(\tau)]} dw_{\tau}^j, \\ t \leq s \leq T & , \quad i = 1, \dots, n, \end{aligned} \quad (A4)$$

$\{dw_{\tau}^i\}_{i=1, \dots, n}$ being independent one-dimensional Wiener differentials (see Appendix B). To model Dirichlet and Neumann boundary conditions it is possible to enforce suitable behaviours of the process ξ at the boundary (Gihman and Skorohod, 1972; Gerardi et al., 1984), i.e., more precisely (see *Fig. 1*):

- Dirichlet boundary condition \Rightarrow *absorption at the boundary*:
a constant value is assigned to the process ξ after reaching the boundary,
 $\xi(t) = \underline{x}_i = \xi(t_{reach})$ for $t > t_{reach}$, $t_{reach} := \sup_t [\xi(t) \in \mathcal{D}]$.
- Neumann boundary condition \Rightarrow *reflection at the boundary*:
the process is reflected normally after hitting the boundary (completely elastic collision, instantaneous reflection), $\xi'(t_{reach}) \rightarrow \xi(t_{reach})$.

³For Dirichlet boundary conditions the function f must be zero at the boundary.

Combinations of absorption and (possibly delayed) reflection can be used to model more complex (mixed) boundary conditions (Gerardi et al., 1984).

On the other hand the parabolic problem (A2) admits an equivalent solution in terms of eigenfunctions expansion (Gelfand and Yaglom, 1960), viz.:

$$\psi(\underline{x}, t, T) = \sum_{j=1}^{\infty} \exp[-\lambda_j(T-t)] (\phi_j, f) \phi_j(\underline{x}), \quad (A5)$$

where (\cdot, \cdot) denotes the inner product in $L^2(R^n)$, viz.:

$$(f, g) := \int_{\mathcal{D}} f(\underline{x}) g(\underline{x}) d\underline{x} \quad , f, g \in L^2(\mathcal{D}), \quad (A6)$$

and the convergence is meant in the $L^2(R^n)$ norm.

By comparing the logarithmic counterpart of eq.s (A3), (A5), at $t = 0$ and two different final times $T = T_1, T_2$, one finally finds:

$$\begin{aligned} \lambda_1 &\sim (T_2 - T_1)^{-1} \log \left[\frac{\psi(\underline{x}, 0, T_1)}{\psi(\underline{x}, 0, T_2)} \right] = \\ &= (T_2 - T_1)^{-1} \log \left\{ \frac{E_{\underline{x}} \left[f[\underline{\xi}(T_1)] \exp \left\{ -\int_0^{T_1} V[\underline{\xi}(s)] ds \right\} \right]}{E_{\underline{x}} \left[f[\underline{\xi}(T_2)] \exp \left\{ -\int_0^{T_2} V[\underline{\xi}(s)] ds \right\} \right]} \right\} \quad , \quad T_2 > T_1. \end{aligned} \quad (A7)$$

The residual error $\epsilon_{res}(\lambda_1)$ affecting eq. (A7) can be easily estimated, viz.:

$$\epsilon_{res}(\lambda_1) = (T_2 - T_1)^{-1} \left| \log \left\{ \frac{1 + \sum_{j>1} \exp[-(\lambda_j - \lambda_1)T_1] \frac{\phi_j(\underline{x}) (\phi_j, f)}{\phi_1(\underline{x}) (\phi_1, f)}}{1 + \sum_{j>1} \exp[-(\lambda_j - \lambda_1)T_2] \frac{\phi_j(\underline{x}) (\phi_j, f)}{\phi_1(\underline{x}) (\phi_1, f)}} \right\} \right|. \quad (A8)$$

This shows that the error can be made in principle as small as one wishes by choosing T_1, T_2 large enough, under the assumption of a strictly increasing eigenvalue sequence. Moreover, one can capitalize on the freedom in the choice of the *weight function* f to further reduce the error. In fact, if one knew (roughly) the behaviour of the principal eigenfunction ϕ_1 , one could choose a weight function f with the same behaviour, and so exploit the orthogonality of the eigenfunctions system to wipe out the higher order terms in the sums involved in eq. (A8), reducing the residual error. A qualitative estimation of the fundamental eigenfunction behaviour (at least its symmetry properties) is generally not very difficult and can highly improve the accuracy. However, at least one has to provide that $\langle \phi_1, f \rangle \neq 0$ and $\phi_1(\underline{x}) \neq 0$ to avoid *jumping* on the second eigenvalue λ_2 .

Following the same basic idea, by comparing eq.s (A3), (A5), at $t = 0$ and a large enough final time T , one can easily estimate the principal eigenfunction:

$$\phi_1(\underline{x}) \sim C\psi(\underline{x}, 0, T) = CE_{\underline{x}} \left[f[\underline{\xi}(T)] \exp \left\{ - \int_0^T V[\underline{\xi}(s)] ds \right\} \right], \quad (A9)$$

C being a suitable normalization constant.

In the presence of a *conservative problem*, e.g. a Neumann-potential-free problem, viz.:

$$\begin{cases} L\phi(\underline{x}) + \lambda\phi(\underline{x}) = 0 & , \quad \underline{x} \in \mathcal{D}, \\ \frac{\partial \phi}{\partial n}(\underline{x}) = 0 & , \quad \underline{x} \in \partial\mathcal{D}, \end{cases} \quad 1 \quad (A10)$$

the principal mode is trivially: $\phi_1 = \text{constant}$, $\lambda_1 = 0$. To compute the lowest non-trivial mode one can cancel the (constant) bias term in the modal expansion (A5) by choosing a zero-area weight function f , namely:

$$\int_{\mathcal{D}} f(\underline{x}) d\underline{x} = 0. \quad (A11)$$

APPENDIX B - ITÔ PROCESSES AND FUNCTIONAL INTEGRALS.

An n -dimensional Itô Process $\underline{\xi} = (\xi^1, \dots, \xi^n)$ of initial point $\underline{x} = (x^1, \dots, x^n)$ is defined as the solution of the stochastic integral equation (Gihman and Skorohod, 1972; Gardiner, 1983):

$$\xi^i(s) = x^i + \int_t^s a^i[\underline{\xi}(\tau)] d\tau + \sum_{j=1}^n \int_t^s \sqrt{b^{ij}[\underline{\xi}(\tau)]} dw_{\tau}^j, \quad (B1)$$

$$t \leq s \leq T, \quad i = 1, \dots, n,$$

$\{dw_{\tau}^i\}_{i=1, \dots, n}$ being independent one-dimensional Wiener differentials (Gardiner, 1983), namely:

$$dw_{\tau}^i = \lim_{\delta \rightarrow 0} \Delta W_i(\delta), \quad (B2)$$

$\Delta W_i(\delta)$ being independent gaussian distributed random variables with means and variances:

$$E[\Delta W_i(\delta)] = 0, \quad E[(\Delta W_i(\delta))^2] = \delta. \quad (B3)$$

It is possible to define a *probability measure* associated to the above process and demonstrate that, for a wide class of regular functionals, there exists an *integral* over it (see Gelfand and Yaglom, 1960; Schulman, 1981). Such an integral admits an immediate interpretation as an *average* of the functional over the process paths (Schulman, 1981).

REFERENCES.

- Collin R.E., 1960, *Field Theory of Guided Waves*, McGraw-Hill, New York.
- Collin R.E., 1992, *Foundations for Microwave Engineering*, McGraw-Hill, New York.
- Donsker M.D. and Kač M., 1950, J. Res. NBS, **44**, p. 551.
- Galdi V., Pierro V. and Pinto I.M., 1997, *Electromagnetics*, **17**, 1, pp. 1-14.
- Gardiner C.W., 1983, *Handbook of Stochastic Methods for Physics, Chemistry and Natural Sciences*, Springer-Verlag, Berlin.
- Gelfand I.M. and Yaglom A.M., 1960, J. Math. Phys., **1**, p. 48.
- Gerardi A., Marchetti F. and Rosa A.M., 1984, System and Control Lett., **4**, pp. 253-261.
- Gihman I.I. and Skorohod A.V., 1972, *Stochastic Differential Equations*, Springer Verlag.
- Harrington R.F., 1968, *Field Computation by Moment Methods*, McMillan, New York.
- Kloeden P.E. and Platen E., 1991, *Numerical Solution of Stochastic Differential Equations*, Springer, New York.
- Ray D., 1954, Trans. Am. Math. Soc., **77**, pp. 299-321.
- Reed M. and Simon B., 1975, *Methods of Modern Mathematical Physics*, II, Academic Press, New York.
- Schulman L.S., 1981, *Techniques and Applications of Path Integration*, J. Wiley & Sons, New York.
- Silvester P.P and Ferrari R.L, 1990, *Finite Elements for Electrical Engineering*, Univ. Press, Cambridge.
- Sobol I.M., 1975, *The Monte Carlo Method*, MIR, Moscow.
- Ventsel A.D., 1983, *Stochastic Processes*, MIR, Moskow.